View metadata, citation and similar papers at core.ac.uk
brought to you by CORE
provided by Repository@Nottingham

The effect of coordination of Alkanes, Xe and CO_2 (η^1-OCO) on Changes in Spin State and Reactivity in Organometallic Chemistry: A Combined Experimental and Theoretical Study of the Photochemistry of $CpMn(CO)_3$

Xue Wu,[1] Zhen Liu,[2] Thomas S. Murphey,[1] Xue Z. Sun,[1] Magnus Hanson-Heine,[1] Jeremy N. Harvey*[3] and Michael W. George*[1,4]

[1]School of Chemistry, University of Nottingham, University Park, Nottingham, NG7 2RD, UK.

[2]State Key Laboratory of Chemical Engineering, East China University of Science and Technology, Meilong Road 130, Shanghai 200237, China.

[3]Department of Chemistry, KU Leuven, Celestijnenlaan 200F, B-3001 Leuven, Belgium.

[4]Department of Chemical and Environmental Engineering, University of Nottingham Ningbo China, 199 Taikang East Road, Ningbo 315100, China.

Abstract

A combined experimental and theoretical study is presented of several ligand addition reactions of the triplet fragment $^3CpMn(CO)_2$ formed upon photolysis of $CpMn(CO)_3$. Experimental data are provided for reactions in *n*-heptane and perfluoromethylcyclohexane (PFMCH) as well as in PFMCH doped with C_2H_6, Xe and CO_2. In PFMCH we find that the conversion of $^3CpMn(CO)_2$ to $^1CpMn(CO)_2$(PFMCH) occurs much slower (τ = 18 (±3) ns) than the corresponding reactions in conventional alkanes (τ = 111 (±10) ps). We measure the effect of the coordination ability by doping PFMCH with alkane, Xe and CO_2; these doped ligands form the corresponding singlet adducts with significantly variable formation rates. The reactivity as measured by the addition timescale follows the order $^1CpMn(CO)_2(C_5H_{10})$ (τ = 270 (±10) ps) > $^1CpMn(CO)_2Xe$ (τ =3.9 (±0.4) ns) ~ $^1CpMn(CO)_2(CO_2)$ (τ =4.7 (±0.5) ns) > $^1CpMn(CO)_2(C_7F_{14})$ (τ = 18 (±3) ns). Electronic structure theory calculations of the singlet and triplet potential energy surfaces and of their intersections, together with non-adiabatic statistical rate theory, reproduce the observed rates semi-quantitatively. It is shown that *triplet* adducts of the ligand and $^3CpMn(CO)_2$ play a role in the kinetics, and account for the variable timescales observed experimentally.

Introduction

Many chemical reactions have elementary steps that involve changes in the total electronic spin. Unravelling the full mechanism of such reactions requires a detailed investigation of the spin changes occurring during the reaction pathway and a combination of experimental and theoretical methods have been used to this end.[1] Metal complexes play key roles as catalysts in a broad variety of chemical and biological processes. In such complexes, ligand association or dissociation at the metal centre can lead to fundamental changes in the coordination sphere of that metal, and these processes obviously also underpin a wide-range of organometallic reactivity. Binding of a ligand can frequently cause a change in spin state by changing the ligand field. Such *"spin-forbidden"* ligand associations can be slower than related spin-allowed ones and this kinetic effect makes this type of process one of the most important spin-forbidden reactions to occur in organometallic chemistry.

$^3Fe(CO)_4$ is one of the most extensively studied model systems for *spin-forbidden* ligand association. In matrices at cryogenic temperatures (12 K) it was shown that UV photolysis of $Fe(CO)_5$ generated $^3Fe(CO)_4$ with an unusual C_{2V} symmetry.[2] In Xe and CH_4 matrices, $^3Fe(CO)_4$ could be converted by near-IR radiation to $^1Fe(CO)_4L$ (L = Xe or CH_4) while analogous experiments[3] performed in more weakly coordinating matrices (Ne or Ar) showed no reaction of $^3Fe(CO)_4$ with the matrix. The photochemistry of $Fe(CO)_5$ has since been investigated in the gas phase and in solution using techniques such as time-resolved IR,[4] time-of-flight mass spectrometery,[5] electron diffraction,[6] X-ray absorption and scattering[7] and XPS.[8] Gas-phase measurements of the kinetics of reaction of $Fe(CO)_4$ with CO, H_2 and other ligands have been reported,[4(c),(d),(f)] showing an effect of the spin-state change in contrast to spin-preserving reactions of $Fe(CO)_3$. We have used picosecond and nanosecond time-resolved infrared (TRIR) spectroscopy[9] in both conventional and supercritical solvents[10] to monitor the reactivity of $^3Fe(CO)_4$ in solvents some of which mirror the original low temperature matrix isolation experiments.[2-3] The formation of $^1Fe(CO)_4$(solvent) was observed when experiments were performed in *n*-heptane, supercritical Xe (scXe), and CH_4 ($scCH_4$).[9] However, experiments carried out using very weakly coordinating solvents, scAr and scKr,[9-10] demonstrated that formation of $^1Fe(CO)_4L$ (L = Ar, Kr) could not be observed following the decay of $^3Fe(CO)_4$ and this observation was consistent with the reported matrix isolation results.[3] Subsequently, we combined experiment and theory[11] to investigate several ligand addition reactions of the triplet fragments $^3Fe(CO)_4$ and $^3Fe(CO)_3$ formed upon photolysis of $Fe(CO)_5$. We used nonadiabatic transition state theory (NATST) to predict rate constants for ligand addition, based on density functional theory (DFT) calculations of singlet and triplet potential energy surfaces[12] and their minimum energy crossing points or MECPs. Interestingly, these calculations suggested a different reaction order in the gas phase[4(c),(d),(f)] and in some condensed phase experiments, due to a change in the rate-determining step from spin-allowed ligand addition to spin-state change in the isolated metal fragment.

There have been many other photoinitiated experimental and theoretical studies on the reactivity of spin-forbidden reactions including investigations on $CpV(CO)_4$ (Cp = η^5-C_5H_5),[13] $CpMn(CO)_3$,[14] Fe $(dmpe)_2$,[15] (dmpe = $Me_2PCH_2CH_2PMe_2$), $Fe(CO)_4$(η^2-1,4-pentadiene),[16] $CpCo(CO)_2$,[17] and (PNP)Co(CO) (PNP = [$^tBu_2PCH_2SiMe_2)_2N]^-$).[18]

Harris and co-workers showed[14] that photolysis of $CpMn(CO)_3$ in neat pentane or Et_3SiH generated $^3CpMn(CO)_2$ followed by formation of respectively $^1CpMn(CO)$(pentane) or $^1CpMn(CO)(Et_3SiH)$; both spin-forbidden processes occurred on similar timescales ($\tau \sim 100$ ps). More recently experiments monitoring photolysis of $CpMn(CO)_3$ in an Ar matrix at 10 K characterised both triplet and singlet $CpMn(CO)_2$. Monitoring the changes in the IR bands of $^3CpMn(CO)_2$ allowed the conversion to $^1CpMn(CO)_2$ to be followed.[19]

In this paper, we exploit the use of perfluorinated solvents which are are valuable for such mechanistic studies because they are very weakly coordinating, and this allows one to examine the effects of doping in more strongly coordinating ligands. Such perfluorous solvents have found use in this way previously,[20] most notably by Kelly and co-workers.[21] Here we will probe the effect of the nature of the weakly coordinating ligand on the spin-change involved in the conversion of $^3CpMn(CO)_2$ to $^1CpMn(CO)_2L$ (L = perfluoromethylcyclohexane, heptane, CH_4, Xe or CO_2) i.e. comparing the effects of heptane vs perfluoromethylcyclohexane vs CH_4 vs CO_2 (η^1-OCO coordination) and Xe. The chemistry of these weakly coordinating ligands has a long history.[22] Organometallic alkane complexes have now been shown to act as reaction intermediates in many fundamental transformations[23] and, in solution, they have been characterised by a range of spectroscopic approaches.[24] Indeed $CpRe(CO)_2$(alkane) was found to be sufficiently long-lived[25(a)] to permit characterisation by NMR.[25(b)] Subsequently a number of other alkane complexes have also been observed using NMR spectroscopy.[26] In the solid state, a well-defined σ-alkane complex was produced following solid/gas single-crystal to single-crystal transformation which allowed the X-ray crystallographic characterisation of $[Rh(R_2PCH_2CH_2PR_2)(\eta^2{:}\eta^2\text{-NBA})][BArF_4]$ {NBA = norbornane; R = ^{i}Bu, or Cy; ArF = 3,5-$(CF_3)_2C_6H_3$)}.[27]

In solution, a W-alkane carbon distance of 3.07 (± 0.06) Å has very recently been determined for $W(CO)_5$(*n*-heptane) using time-resolved XAFS.[28] The measured distance was longer than that calculated for binding to the primary C-H group (2.86 Å), but shorter than that calculated for interaction with the secondary C-H group W-C (3.12 Å). Overall, the measured value is consistent with statistical averaging of the values for the primary and secondary C-H groups, suggesting that the XAFS measurements reflect an equilibrating ensemble in which the metal fragment coordinates to the different C-H bonds, which would be consistent with 'alkane chain walking' by the $W(CO)_5$ fragment. A stable metal-xenon complex has also been reported following reduction of AuF_3 with elemental xenon in HF/ SbF_5 solution, resulting in the formation of $[AuXe_4]^{2+}[Sb_2F_{11}]^{2-}$ characterised by X-ray crystallography.[29] The use of perfluoroalkanes doped with Xe allowed the generation of organometallic xenon complexes at room temperature in conventional fluids without the need to use high-pressure liquefied or supercritical Xe solvents.

In solution the generation of organometallic noble gas complexes have been characterised following photolysis of a metal carbonyl precursor in high-pressure liquid or supercritical noble gas solutions.[30] For a given metal carbonyl moiety, it has generally been found that the organometallic Xe complexes were roughly twice as reactive than the corresponding organometallic alkane complexes.[31] In liquefied Xe at cryogenic temperatures, $PrCpRe(CO)(PF_3)Xe$ (^{i}PrCp = η^5-C_5H_4-$CH(CH_3)_2$) had a sufficiently long lifetime to be observed using NMR.[32] Like for alkanes, the coordination of CO_2 to transition metal centres is of interest because it is a key step in many reactions

and catalytic processes. CO_2 has been observed to have three different binding modes (carbon-bound η^1-C, side-on bidentate η^2-C,O, and end-on oxygen-bound η^1-O).[33] Several examples of η^1-C and η^2-C,O CO_2 complexes have been isolated, and their modes of CO_2 coordination have been confirmed by X-ray crystallography. By contrast, the η^1-OCO coordination mode has mainly been predicted theoretically and deduced from spectra obtained in low-temperature matrices. One example has been characterized crystallographically,[34] $(AdArO)_3tacn)U^{IV}(CO_2)$ {$(AdArOH)_3tacn$) = 1,4,7-tris(3-adamantyl-5-tert-butyl-2-hydroxy- benzyl)1,4,7-triazacyclononane)} We reported the characterization of η^1-OCO organometallic complexes in solution at room temperature by characterising $M(CO)_5(CO_2)$ (M = Cr, Mo, or W) and $CpMn(CO)_2(CO_2)$ in $scCO_2$ using fast time-resolved infrared spectroscopy (TRIR).[35] For Mn, this conclusion was based on a combination of DFT calculations and the relative wavenumbers of the ν(C-O) IR bands of $CpMn(CO)_3$ and $CpMn(CO)_2(CO_2)$ and indicating that CO_2 was most probably binding to Mn via an η^1-OCO coordination mode. The relative reactivities of $CpMn(CO)_2L$ (L= *n*-heptane, CH_4, Xe or CO_2) towards CO were shown to lie in the order *n*-heptane < CH_4 < Xe $\sim$ CO_2).[36] In this paper, we investigate the effect of the binding of weakly coordinating ligands on the spin-change involved in the reactions of $^3CpMn(CO)_2$ to form $^1CpMn(CO)_2L$ and utilise perfluoroalkanes doped with Xe or CO_2 to allow the reactivity of these ligands to be explored. As well as experimental approaches, DFT calculations, benchmarking correlated *ab initio* results, and NATST rate constant calculations are reported.

Experimental and Computational Details

$CpMn(CO)_3$ (Strem), Xenon (BOC, >99.99%), methane (BOC, >99.99%), ethane (Air products, > 99.95%), and CO_2 (BOC, > 99.99%) were used without further purification. Perfluoro(methylcyclohexane) (Alfa Aesar) and *n*-heptane (Aldrich) were refluxed over CaH_2 under an inert argon atmosphere prior to use. $CpRf^{21}Mn(CO)_3$ ($Rf^{21}Cp$ = $(C_6F_{13}CH_2CH_2)C_5H_5$) were prepared by reaction of the fluorinated cyclopentadienyl anion with $Mn(CO)_5Br$ following the reported procedure.[37]

The TRIR experiments were performed either at Nottingham or at the ULTRA facility at the Rutherford Appleton Laboratory, which have been discussed in detail elsewhere[38-39] and therefore, only a brief summary is given here. At Nottingham 800 nm laser pulses (100 fs, 1 kHz) were generated with a commercial Ti:sapphire oscillator (MaiTai) / regenerative amplifier system (Spitfire Pro/Spectra Physics, USA). The 800 nm laser beam was divided into two parts with approximately equal energy. One part pumps a TOPAS-C OPA (Light Conversion, Lithuania) to produce tunable UV-Vis-NIR pulses (300 nm - NIR) for pumping. Another part pumps a second TOPAS-C OPA with a Difference Frequency Generator (DFG) unit to produce tunable mid-IR pulses (2.5-10 μm) as a probe beam. The IR beam passes through a Ge beam splitter so that half of IR beam is reflected onto a single element MCT detector (Kolmar Technology) to serve as a reference and the other half, passing through the Ge beam splitter is focused and overlaps with the pump beam at the sample position. The UV-Vis pump pulse was optically delayed (up to 3 ns) by a 1 meter translation stage (LMA Actuator, Aerotech, USA), and focused onto the sample with a quartz lens. The polarization of the pump pulse was set at the magic angle (54.7^o) relative to the probe pulse to recover the isotropic absorption

spectrum. For a measurement with a longer time delay, a Q-switched Nd:YVO laser (ACE- 25QSPXHP/MOPA, Advanced Optical Technology, UK) was employed as a pump source which is synchronized to the Spitfire Pro amplifier. The IR probe beam was dispersed with a spectrograph and detected with a N_2(l)- cooled HgCdTe linear array detector (Infrared Associates, USA) which consists of 128 elements (1 mm high, 0.25 mm wide).

At the Rutherford laboratory, a Ti:sapphire laser amplifier (Thales Laser) produces 800 nm laser pulses (0.8 mJ, 10 kHz with a pulsewidth of 50 fs). This laser output is split, and one portion is used to generate the 267 nm pump beam by harmonic generation. The second portion is sent through an optical parametric amplifier (Light Conversion) and a difference frequency generator to produce a tunable mid-IR probe. The diameter of the pump and probe beams were around 150 and 80 µm, respectively. After transmission through the sample, the IR probe is dispersed onto two linear 128 element MCT detector arrays (Infrared Associates). By the use of a chopper, the pump-on and pump-off infrared intensities can be measured, and difference spectra generated. A small portion of the IR probe beam is taken before the sample and dispersed onto a 64 element MCT detector array (Infrared Associates) to provide a reference signal for beam intensity fluctuations. In both experimental set-ups, the sample solution flows through a Harrick cell which was mounted on a motorized cell mount rapidly moving in x and y dimensions and continuously in a plane perpendicular to the beam direction along the z-axis.

Dispersion corrected DFT calculations were carried out using the Gaussian 09 package[40] together with flexible basis sets (Def2SVP and Def2TZVP) of Ahlrichs *et al*.[41] Most DFT calculations were performed using the B3LYP** functional, which is a modified form of the B3LYP functional as implemented in Gaussian, in which the percentage of the exact Hartree-Fock exchange energy has been reduced from 20% in the standard B3LYP to 10% in order to predict more trustable splitting energies between two adjacent spin states. The structures of the $CpMn(CO)_2$ fragment in the singlet and triplet states were optimized at the B3LYP**-D3BJ/Def2TZVP level, and the zero-point energy corrections and Gibbs free energy corrections were obtained from frequency calculations at the same level of theory. For the interaction with ligands Xe, CO_2, C_2H_6, C_7H_{16}, C_6F_{12}, and C_7F_{14}, we first carried out a thorough conformational search for triplets and singlet at the B3LYP**-D3BJ/Def2SVP level of theory. For all ligands except the perfluoroalkanes, the structures of all conformers were then refined at the B3LYP**-D3BJ/Def2TZVP level, and frequencies computed. For the perfluoroalkanes, due to the large number (> 50) of conformers, only low-energy structures from optimization at the B3LYP**-D3BJ/Def2SVP level were refined. Minimum energy crossing points (MECPs) between singlet and triplet potential energy surfaces were also located at the B3LYP**-D3BJ/def2TZVP level of theory by using the code developed by Harvey and Aschi.[42] Free energies have been computed using the quasi-harmonic approach,[43] whereby small real or imaginary frequencies with magnitudes below 20 cm^{-1} were treated as being equal to 20 cm^{-1}. Finally, rate coefficients for the spin-forbidden reactions were calculated using MESMER program,[44] based on the properties of the MECPs calculated with B3LYP** and on the root-mean square singlet-triplet spin-orbit coupling constant of 168 cm^{-1} at the MECP for the $CpMn(CO)_2$ system calculated based on state-averaged singlet and triplet CASSCF(10,10) wavefunctions with a cc-pwCVTZ basis on Mn

and aug-cc-pVDZ basis sets on other atoms. These calculations were performed with the MOLPRO 2012 program package.[45]

Results and Discussion

As stated above, Harris and co-workers identified the short-lived coordinatively-unsaturated triplet intermediate $^3CpMn(CO)_2$ during picosecond time-resolved IR (TRIR) investigations of the photolysis of $CpMn(CO)_3$ in *n*-heptane and triethylsilane solvents. This triplet intermediate was shown to decay to form the singlet solvent complex $^1CpMn(CO)_2$(solvent) (solvent = *n*-heptane or Et_3SiH). Before examining the photochemistry of $CpMn(CO)_3$ in perfluorinated solvents, we repeated the previous work[14] in an alkane solvent particularly as no data in alkane were presented for comparison. Figure 1 shows the TRIR difference spectra recorded following photolysis (266 nm) of $CpMn(CO)_3$ in n-heptane. It is clear from the spectrum obtained 1 ps after excitation that the parent ν(C-O) bands are bleached and two new broad ν(C-O) bands are formed at ca. 2000 and 1846 cm^{-1}. These new ν(C-O) bands sharpen and blue-shift to 2004 and 1849 cm^{-1} over the first 5-10 ps following excitation which is consistent with vibrational cooling of the initially formed transient. These bands are assigned to $^3CpMn(CO)_2$ by comparison with the previous TRIR and matrix isolation studies, see Table 1

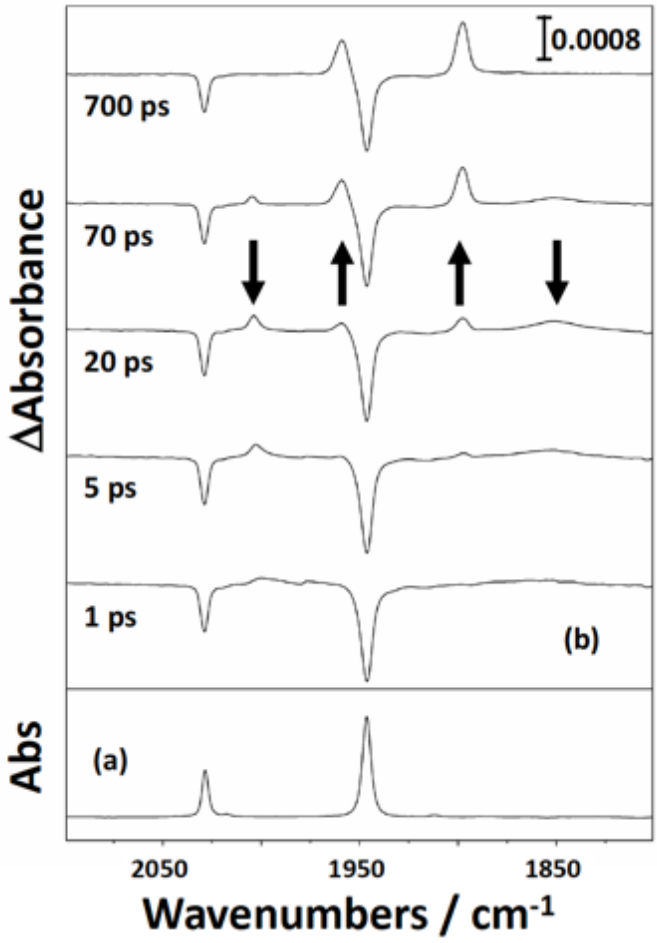

Figure 1 *(a) FTIR of a solution of $CpMn(CO)_3$ in n-heptane and (b) Selected picosecond TRIR spectra recorded at a series of ime delays following 266 nm photolysis of this solution.*

Table 1: *ν(C-O) IR band positions of $CpMn(CO)_3$ and intermediates produced following photolysis in either a range of solvents at room temperature or in an Ar matrix at 10 K.*

Compound	Solvent or Matrix	ν(C-O)	Reference
$CpMn(CO)_3$	*n*-heptane	2028, 1946	This work
$CpMn(CO)_3$	PFMCH	2033, 1952	This work
$CpMn(CO)_3$	Triethylsilane	2028, 1947	14
$CpMn(CO)_3$	Ar matrix	2032, 1948	19
$^3CpMn(CO)_2$	*n*-heptane	2004, 1849	This work
$^3CpMn(CO)_2$	PFMCH	2008, 1850	This work
$^3CpMn(CO)_2$	Triethylsilane	2002, 1883	14
$^3CpMn(CO)_2$	Ar matrix	2006, 1853	19
$^1CpMn(CO)_2$(solvent)	*n*-heptane	1960, 1897	This work
$^1CpMn(CO)_2$(solvent)	PFMCH	1965, 1895	This work
$^1CpMn(CO)_2$(solvent)	Triethylsilane	1960, 1892	14
$^1CpMn(CO)_2$	Ar matrix	1973, 1904	19

The two ν(C-O) bands of $^3CpMn(CO)_2$ decay at the same rate (τ = 111 (±10) ps) as the organometallic alkane complex, $^1CpMn(CO)_2(n\text{-}C_7H_{16})$, is formed, Figure 2. These results are consistent with the original observation by Harris and co-workers.[14] Experiments were repeated in cycloheptane as a solvent and similar results were observed with the conversion of $^3CpMn(CO)_2$ to $^1CpMn(CO)_2(c\text{-}C_7H_{16})$ occurring with a slightly faster rate. It has been previously shown that cyclic alkanes form more stable interactions with metal centres and this stronger interaction may be contributing to the slightly faster spin crossover.

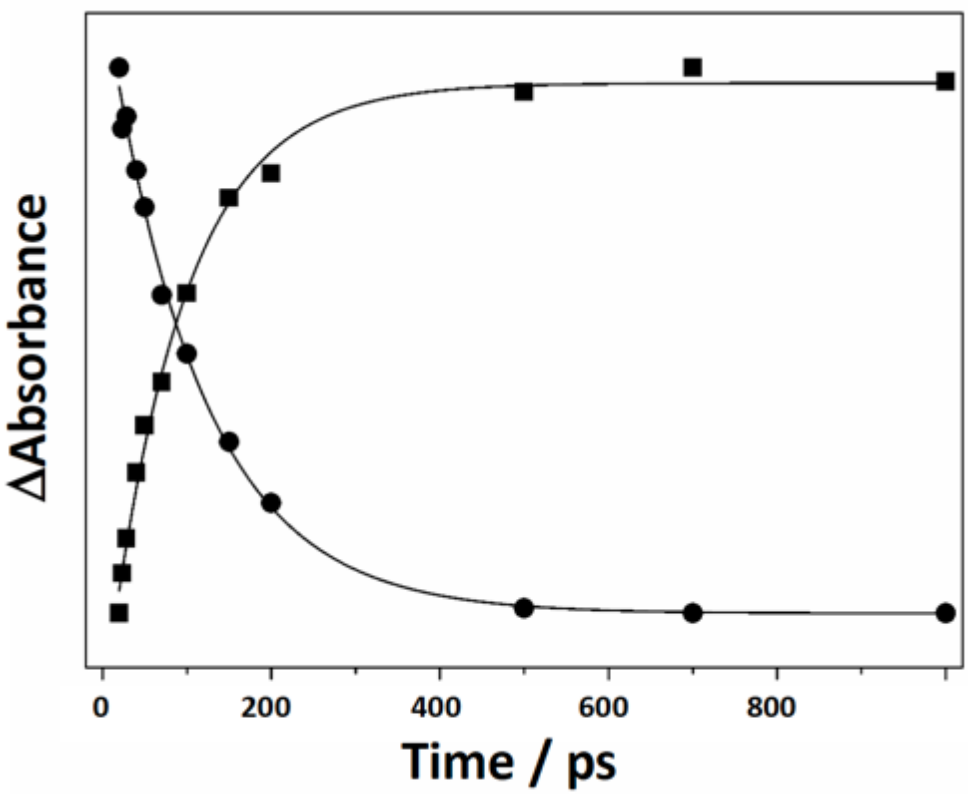

Figure 2 *TRIR Kinetic traces obtained from the spectra recorded following 266 nm irradiation of $CpMn(CO)_3$ in n-heptane solution showing the decay of $^3CpMn(CO)_2$ at 2004 cm^{-1} (circles) and growth of $^1CpMn(CO)_2(C_7H_{16})$ at 1897 cm^{-1}(squares).*

Following the experiments in pure alkane solvents described above, we investigated the photochemistry of $CpMn(CO)_3$ in perfluoromethylcyclohexane (PFMCH). Figure 3 shows the TRIR spectra recorded following excitation (266 nm) of $CpMn(CO)_3$ in PFMCH. The TRIR spectrum obtained after 1 ps is similar to the spectrum in *n*-heptane; bands of the parent complex are depleted and two new broad ν(C-O) bands are produced. These bands again appear vibrationally hot, and cool over ca. 30 ps to yield bands at 2007 and 1848 cm^{-1}. It can be noted that this cooling process is much slower than that observed for the corresponding process in *n*-heptane. These two ν(C-O) bands are assigned to the unsaturated triplet species, $^3CpMn(CO)_2$ in PFMCH. Interestingly, the triplet complex is much more stable in PFMCH than in heptane and can still be observed on the nanosecond timescale.

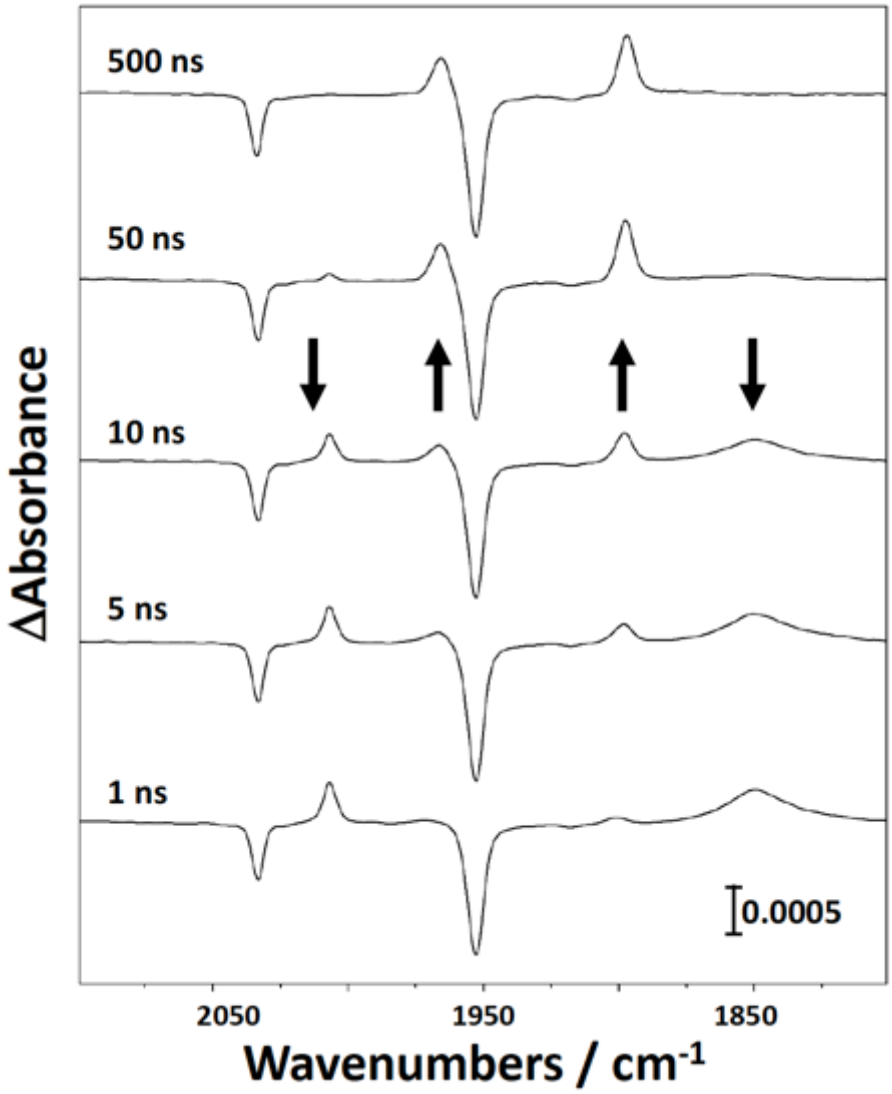

Figure 3 *Selected nanosecond TRIR spectra recorded at a series of time delays following 266 nm photolysis of a solution of $CpMn(CO)_3$ in PFMCH.The decay of the ν(CO) bands of $^3CpMn(CO)_2$ at 2007 $cm^{-1}$and growth of those corresponding to $^1CpMn(CO)_2(C_7F_{14})$ at 1965 cm^{-1}.*

$^3CpMn(CO)_2$ decays (τ = 18 (±3) ns) to form a new species with ν(CO) bands at 1965 and 1879 cm^{-1} which are slightly higher than those in $^1CpMn(CO)_2$(*n*-heptane), and are assigned to $^1CpMn(CO)_2(C_7F_{14})$, Figure 3. The rate for this process is two orders of magnitude slower than those observed in *n*-heptane or *c*-pentane, possibly due to a weaker interaction between the PFMCH solvent and the Mn centre and these differences will be discussed in more detail later.

We have repeated the above experiment using $CpRf^{21}Mn(CO)_3$ ($Rf^{21}Cp$ is the substituted cyclopentadienyl ring $(C_6F_{13}CH_2CH_2)C_5H_5$) and again observed conversion from $^3CpRf^{21}Mn(CO)_2$ to $^1CpRf^{21}Mn(CO)_2(C_7F_{14})$ occurring on the nanosecond timescale (τ = 5.9 (±0.2) ns). Assuming that alkanes are bonded more strongly than PFMCH to the metal centre, doping a small amount of alkane into the PFMCH solvent should change the rate of formation of the singlet complex $^1CpMn(CO)_2X$ (X = solvent or dopant), as well as its ν(CO) band positions. Thus, a selection of picosecond TRIR spectra obtained following photolysis (266nm) of $CpMn(CO)_3$ in 10:1 PFMCH:*c*-pentane are shown in Figure 5. These spectra show that photolysis initially generated $^3CpMn(CO)_2$, in a vibrationally excited state and that the ground state IR ν(CO) bands of $CpMn(CO)_3$ and $^3CpMn(CO)_2$ appear to be unaffected by the addition of *c*-pentane to the PFMCH solvent. However, in these doped experiments, the bands of $^3CpMn(CO)_2$ begin to decay on a picosecond timescale, concurrently with formation of two ν(CO) bands at 1963 and 1896 cm^{-1} (τ = 270 (±10) ps) which are shifted relative to $^1CpMn(CO)_2(C_7F_{14})$ and are assigned to preferential formation of $^1CpMn(CO)_2(C_5H_{10})$. The rate of this spin-forbidden formation of $^1CpMn(CO)_2(C_5H_{10})$ is indeed close to that observed in pure alkane.

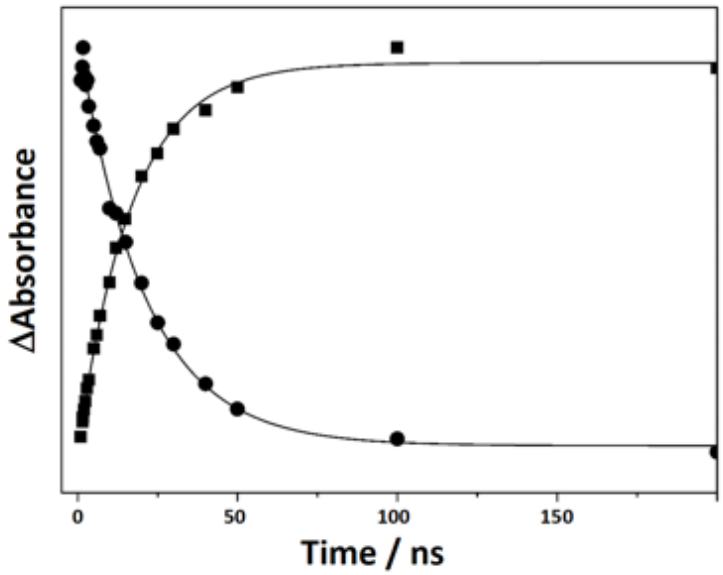

Figure 4: *TRIR kinetic traces obtained following irradiation (266 nm) $CpMn(CO)_3$ in PFMCH solution showing the decay of $^3CpMn(CO)_2$ at 2007 cm^{-1} (circles) and growth of $^1CpMn(CO)_2(C_7F_{14})$ at 1898 cm^{-1} (squares).*

We now investigated whether such preferential binding can be observed for the formation of the previously characterised complexes $CpMn(CO)_2(C_2H_6)$,[9, 26(j)] $CpMn(CO)_2Xe$[30(c)] and $CpMn(CO)_2(CO_2)$[35] by repeating the TRIR experiments and monitoring the photolysis of $CpMn(CO)_3$ in PFMCH doped with 1 atm. of either C_2H_6, Xe or CO_2. Our aim was to see how the binding of these weak ligands affects the spin forbidden reactions of $^3CpMn(CO)_2$ especially as all of these complexes have been shown to be more reactive (less stable) than $^1CpMn(CO)_2(C_5H_{10})$. In all cases we see initially the formation of $^3CpMn(CO)_2$ which then decays to form $^1CpMn(CO)_2L$ (L = C_2H_6, Xe or CO_2), Figure 5. The observed positions of the ν(CO) bands are shown in Table 2.

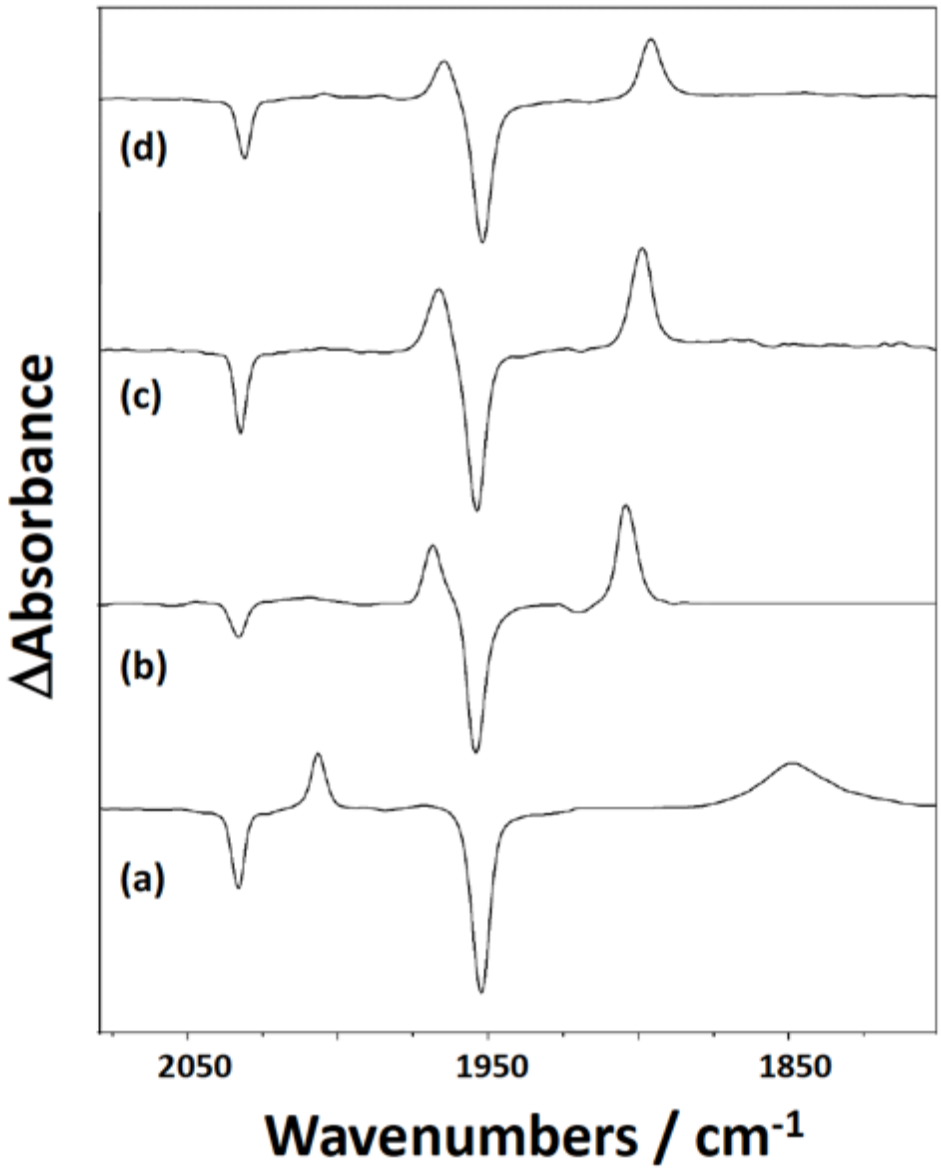

Figure 5 Showing TRIR of $CpMn(CO)_3$ in PFMCH doped with C_2H_6 (a) 1ns and (b) 1 ms following irradiation. The remaining spectra show results from TRIR experiments obtained 1 μs after photolysis (266 nm) of $CpMn(CO)_3$ in PFMCH doped with (c) Xe and (d) CO_2.

Table 2: *ν(C-O) IR band positions of $CpMn(CO)_3$ and intermediates produced following photolysis of $CpMn(CO)_3$ in pure PFMCH or PFMCH doped with c-pentane, Xe, CO_2, CH_4 or C_2H_6.*

Compound	**Dopant**	**ν(C-O) cm^{-1}**
$CpMn(CO)_3$	None	2033, 1952
$CpMn(CO)_3$	*c*-pentane	2033, 1952
$CpMn(CO)_3$	CH_4	2033, 1952
$CpMn(CO)_3$	C_2H_6	2033, 1952
$CpMn(CO)_3$	Xe	2033, 1952
$CpMn(CO)_3$	CO_2	2033, 1952
$^3CpMn(CO)_2$	None	2008, 1950
$^3CpMn(CO)_2$	*c*-pentane	2008, 1950
$^3CpMn(CO)_2$	CH_4	2008, 1950
$^3CpMn(CO)_2$	C_2H_6	2008, 1950
$^3CpMn(CO)_2$	Xe	2008, 1949
$^3CpMn(CO)_2$	CO_2	2008, 1950
$^1CpMn(CO)_2$ (PFMCH)	None	1965, 1897
$^1CpMn(CO)_2$(*c*-pentane)	*c*-pentane	1963, 1896
$^1CpMn(CO)_2(CH_4)$	CH_4	1965, 1897
$^1CpMn(CO)_2(C_2H_6)$	C_2H_6	1964, 1896
$^1CpMn(CO)_2Xe$	Xe	1967, 1898
$^1CpMn(CO)_2(CO_2)$	CO_2	1964, 1896

In all cases, the observed rate at which the triplet $^3CpMn(CO)_2$ undergoes the spin-forbidden reaction to form the solvent complex $^1CpMn(CO)_2L$ in the mixed solvent system is much faster than the rate observed in the pure perfluoroalkane, Figure 6. The order of reactivities for the formation of $^1CpMn(CO)_2L$ is $^1CpMn(CO)_2(C_5H_{10})$ (τ = 270 (±10) ps) > $^1CpMn(CO)_2Xe$ (τ = 3.9 (±0.4) ns) ~ $^1CpMn(CO)_2(CO_2)$ (τ =4.7 (±0.5) ns) > $^1CpMn(CO)_2(C_7F_{14})$ (τ = 18 (±3) ns).

Table 3. *Calculated energies (ΔE / kcal mol^{-1}, including zpe correction) and free energies (ΔG / kcal mol^{-1}, 298 K) for singlet and triplet adducts of various solvents to $CpMn(CO)_2$ as well as for the singlet/triplet MECPs. In all cases, the reference is the ligand free $^3CpMn(CO)_2$ + ligand.*

		/	Xe	CO_2	C_2H_6	hept	pFCyc	pFMCH
	$^1CpMn(CO)_2$•(L)	2.2	-8.5	-8.8	-10.7	-13.3	-5.9	-5.9
Δ*E*	MECP•(L)	3.6	-0.1	-0.9	-1.0	-5.5	-0.3	-0.5
	$^3CpMn(CO)_2$•(L)	0.0	-4.3	-4.5	-3.2	-6.7	-5.3	-5.7
	$^1CpMn(CO)_2$•(L)	3.8	-1.5	-1.0	-1.2	-3.2	3.2	4.7
Δ*G*	$^3CpMn(CO)_2$•(L)	0.0	-0.5	0.4	2.1	1.1	1.2	2.1

Calculated relative energies are shown in Table 3. As can be seen, B3LYP** predicts a triplet ground state for $^3CpMn(CO)_2$ (no ligand), with the singlet lying just higher in energy. We have found elsewhere that B3LYP** is reasonably accurate for predicting the relative spin-state energies of $Fe(CO)_4$ and assume

that this also applies here. Both complexes have C_S symmetry, with the triplet form planar at manganese, while the singlet is pyramidal (sum of angles at Mn between the Cp centroid and the two CO carbon atoms are respectively of 360° and 340.2°), presumably as this allows better back-bonding from the two doubly-filled 3d orbitals. The increased back-bonding in the singlet is also confirmed by the Mn-C (1.827 and 1.789 Å, respectively, in the triplet and singlet states) and C-O bond lengths (1.153 and 1.157 Å). These bond length changes are consistent with the measured vibrational frequencies (2008 and 1950 cm^{-1} for the unligated triplet, 1967 and 1898 cm^{-1} for the singlet xenon complex). Calculated harmonic frequencies match these trends (2035 and 1947 cm^{-1} for the unligated triplet, 2016 and 1962 cm^{-1} for the unligated singlet, vs. 2007 and 1955 for the Xe complex).

Heptane and ethane bind quite strongly to the singlet fragment, with xenon and CO_2 having interaction energies of medium strength, and the perfluoroalkanes interacting most weakly. The binding occurs with close Mn—ligand contacts (e.g. r(Mn-Xe) = 2.787 Å) but does not lead to a large increase in the pyramidalization at Mn (the sum of the same angles as mentioned above drops from 340.2° in the free complex to 338.5° in the Xe complex). We find that all the ligands also form relatively strongly bound complexes with the *triplet* fragment. In most cases, this is due to a mixture of weak two-centre three-electron interactions with the metal itself, and to non-specific van der Waals interactions. The weakness of the interactions with the metal can be seen from the structures, with e.g. a long Mn—Xe distance of 3.854 Å and a sum of angles at Mn remaining at 360°. All optimized structures are included in the Supporting Information. Table 3 also shows the calculated energies for the MECPs between the singlet and triplet states, both with and without the various ligands. These will be discussed below. Finally, Table 3 contains calculated standard free energies for addition, which more or less follow the trend of the potential energies, with less favourable binding due to the entropic penalty. Imperfections of our computational protocol can be seen from the fact that none of the singlet adducts is much more stable than separated $^3CpMn(CO)_2$ and ligand, and for the perfluorinated solvents, the adducts are predicted to be *less* stable than these fragments. These discrepancies may be due to errors in either the description of the spin-state energetics or of the bonding with B3LYP**.

In our first detailed study of the rate of addition of a ligand, CO, to a high-spin metal centre, $^3Fe(CO)_4$, we suggested[46] a concerted addition mechanism (**A** in Figure 6), in which the ligand binding to the metal center, and the spin state change at the metal site, occur in a single step. Using this proposed mechanism, acceptable agreement was obtained between the predicted rate constant and the results of gas-phase experimental kinetics studies,[4(c),(d),(f)] both in terms of the predicted rate constant, the rate law, and the experimentally observed but very small activation energy.

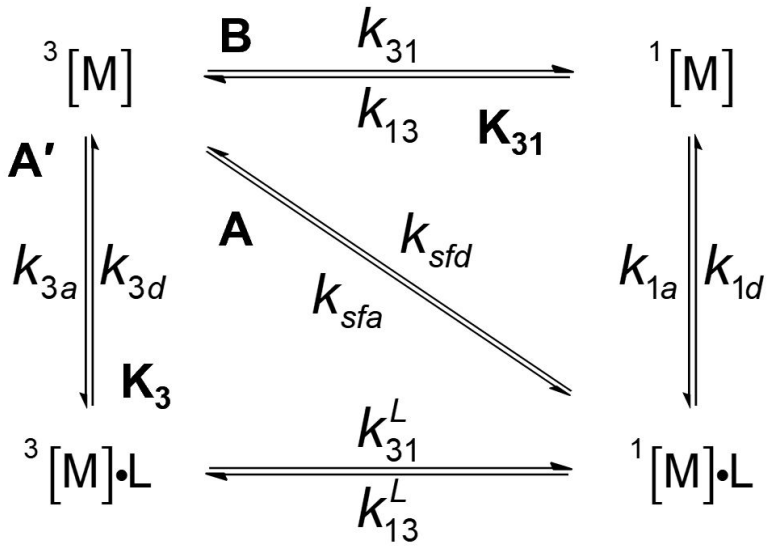

Figure 6 *Proposed reaction mechanisms for ligand addition to triplet metal fragment ^{3}[M] to form singlet bound complex ^{1}[M]•L. (A) Direct pathway with ligand addition and spin state change occurring in a single step; (A') stepwise pathway with ligand addition followed by spin state change; (B) stepwise pathway with spin state change followed by ligand addition.*

Nevertheless, as mentioned in the Introduction, it later became apparent that the concerted mechanism **A** cannot fully account for the kinetics of ligand addition to iron tetracarbonyl because, for the case of reaction with dihydrogen, a high barrier to addition was calculated[47] which is inconsistent with the observed quite large rate constant, also from gas-phase studies.[4(c),(d),(f)] Stepwise mechanism **B**, in which initial spin-state change is followed by spin-allowed addition of dihydrogen yields much better agreement with experiment both in the gas phase and in solution,[11] including accounting for the different rate law in these two cases. Indeed, ligand addition is rate limiting in the dilute gas phase, whereas spin-state change is limiting in solution. Accordingly, in ref. 11, we concluded that mechanism **B** with a fast pre-equilibrium between the two spin states of the metal fragment probably also accounts for much of the rate even for addition of carbon monoxide, though some role for mechanism **A** could not be ruled out.

Although mechanism **B** is successful in accounting for the different behaviour in the gas phase and in solution, and qualitatively reproduces observed rates, it does not account for the fact that in solution, different ligands add to $^3Fe(CO)_4$ at different rates, with e.g. addition of heptane occurring roughly 3 times faster than addition of xenon.[10,11] With mechanism **B** in solution, the observed rate constant for addition should be equal to k_{31} for *all* ligands. At the time, the small differences in observed rate were assumed to be due to small changes in the potential energy surfaces in the different solvents, perhaps due to second-ligand-sphere interactions between the CO ligands and the solvent. However, the larger range in rates observed here with $CpMn(CO)_2$ (by a factor of over 100 from PFCMH to heptane) forces us to refine the

mechanistic framework still further, by allowing for an intermediate mechanism (**A'** in Figure 6) where the triplet metal fragment can add a ligand to form ^{3}[M].L, which can then undergo a spin state change. As discussed below, including this possibility results in a model that accounts reasonably well for the observed reactivity.

In Table 4, we show the rate constants at 298 K for all the elementary steps shown in Figure 6, calculated based on the results of our DFT calculations. Some points need to be mentioned here. First, while the experimental results refer to ligands doped in liquid perfluorinated solvent, our calculations refer to reactions in pure liquid or supercritical fluid. This leads to slight over-prediction of bimolecular rates, but most likely within the error bars of the computation. Next, when calculating standard free energies, we have chosen a standard state that corresponds to the pure fluid for all liquids or supercritical fluids, and this also means that bimolecular rate constants for addition of solvent implicitly contain the solvent concentration, so are expressed as pseudo-unimolecular rate constants in s^{-1} units. For supercritical gases, we have used a standard state concentration that is appropriate for the gas density used in the experiments here (Xe: 8.4 mol dm^{-3}; CO_2: 10.7 mol dm^{-3}; C_2H_6: 6.8 mol dm^{-3}). Next, a number of steps, for addition of solvent to metal fragments, are expected to be diffusion-limited. For a number of cases, we have checked that the potential energy of the system increases monotonically upon progressively pulling the solvent molecule away from the metal. In line with our previous experience,[48-49] we have simply assumed that these steps are indeed diffusion-controlled. Rather than use explicit transition state theory approaches, we have used a simple expression for the rate constants of diffusion-controlled reactions, i.e. $k = 8k_BT/3\eta$, where η is the viscosity, using values, in units of 10^{-3} N s m^{-2}, of 0.05 (Xe, CO_2, and C_2H_6), 0.376 (heptane) and 1.665 (PFMCH and C_6F_{12}). This yields a bimolecular rate constant, which we multiplied by the corresponding concentration to obtain a pseudo-first order rate constant, as discussed above. Finally, under experimental conditions, the singlet solvated adducts ^{1}(M)L are all observed to be stable on the timescale monitored. It therefore appears that ligand *dissociation* from the singlet adduct is not rapid, and for this reason, we have not considered this step.

Table 4. *Calculated rate constants (s^{-1}) relating to addition of Xe, CO_2, C_2H_6, C_7H_{16}, C_6F_{12}, C_7F_{14} to $CpMn(CO)_2$ at 298 K. Also shown are predicted overall rate constants k_{app} for mechanisms **B** and **A'**, and experimental 'rate constants' derived from the TRIR timescales, for Xe, CO_2, heptane and C_7H_{14}.*

	Xe	CO_2	C_2H_6	C_7H_{16}	C_6F_{12}	C_7F_{14}
k_{13}	2.8×10^{12}	2.8×10^{12}	2.8×10^{12}	2.8×10^{12}	2.8×10^{12}	2.8×10^{12}
k_{1a}	1.1×10^{12}	1.4×10^{12}	9.0×10^{11}	1.3×10^{11}	2.2×10^{10}	2.0×10^{10}
k_{31}	4.9×10^{9}	4.9×10^{9}	4.9×10^{9}	4.9×10^{9}	4.9×10^{9}	4.9×10^{9}
$K_{31} \times k_{1a}$	2.0×10^{9}	2.5×10^{9}	1.6×10^{9}	2.2×10^{8}	4.0×10^{7}	3.6×10^{7}
K_3	2.3533	0.5082	0.0295	0.1535	0.1258	0.0302
k_{3d}	4.7×10^{11}	2.8×10^{12}	3.1×10^{13}	8.2×10^{11}	1.8×10^{11}	6.7×10^{11}

k_{31}^{L}	8.0×10^{8}	4.1×10^{9}	5.0×10^{10}	6.3×10^{11}	4.1×10^{8}	2.4×10^{8}
k_{3a}	1.1×10^{12}	1.4×10^{12}	9.0×10^{11}	1.3×10^{11}	2.2×10^{10}	2.0×10^{10}
$K_3 \times k_{31}^{L}$	1.9×10^{9}	2.1×10^{9}	1.5×10^{9}	9.7×10^{10}	5.2×10^{7}	7.3×10^{6}
k_{app} (**B**)	2.0×10^{9}	2.5×10^{9}	1.6×10^{9}	2.2×10^{8}	4.0×10^{7}	3.6×10^{7}
k_{app} (**A'**)	1.9×10^{9}	2.1×10^{9}	1.5×10^{9}	9.7×10^{10}	5.2×10^{7}	7.3×10^{6}
k_{app} (exp)	2.6×10^{8}	2.1×10^{8}	/	9.7×10^{9}	/	5.6×10^{7}

A first important point to make about these calculated rate constants is that some of them are very large indeed – many are above 10^{11} s^{-1}, and a few are larger than 10^{13} s^{-1}. Such large values mean that the implied lifetime for the species prior to reaction is of the order of picoseconds. Even for lifetimes of 10 ps (rate constants of 10^{11} s^{-1}), equilibration of internal vibrational energy with solvent is no longer complete in many cases[49] (as also shown by the observed rates of thermalization reported here) while for lifetimes of 0.1 ps (rate constants of 10^{13} s^{-1}), it is no longer possible to talk of 'species' since this is shorter than the vibrational period of some motions. Clearly, we are at the limit of what can be discussed using transition state theory and the assumption that species are at thermal equilibrium with solvent. One consequence of this is that for some of the reactions considered here, there is in fact no sharp demarcation between mechanisms **A'** and **B**. For example, in mechanism **B**, with initial spin-state change of the triplet metal fragment followed by solvent addition, a very large value for k_{1a} implies that solvent addition to the singlet occurs concomitantly with its formation. From the point of view of mechanism **A'**, with initial addition of solvent on the triplet surface, followed by spin state change in the adduct, a very large rate constant for spin state change k_{31}^{L} implies that this change starts while the ligand is still adding to the metal. In both cases, one really then has a concerted mechanism, more like mechanism **A**, and at the very least, this means that the two mechanisms cannot really be considered as separate. This aspect will be discussed further below.

In order to analyze the elementary step rate constants and to compare with experiment, it is necessary to first analyze which step is predicted to be rate-limiting in each mechanism, and then to consider which of the two mechanisms is predicted to be favoured. For mechanism **B**, if the initial spin-state change is rate-limiting, then the observed rate constant is simply k_{31}. If the second step is rate-limiting, then the observed rate constant would be $K_{31} \times k_{1a}[L]$, or, since the concentrations are implicit in the values for the rate and equilibrium constants, simply $K_{31} \times k_{1a}$. To decide which step is rate-limiting, we compare k_{13} and k_{1a}, the two rate constants relevant to the disappearance of the singlet metal intermediate. If the former is smaller, then the first step is rate-limiting, whereas if the latter is smaller, then the second step is rate-limiting. For accurate results, one would need to consider that for some cases,

both steps could be partially rate-limiting, but this is not needed for the present mainly qualitative purposes. Examination of Table 4 shows that the second step is predicted to be rate-limiting in all cases for the $CpMn(CO)_2$ reactons treated here. This is different from what was predicted[47] for $Fe(CO)_4$, with the difference arising because the MECP is much higher in energy for $Fe(CO)_4$ (6.3 kcal mol^{-1}, ref. 11) than for $CpMn(CO)_2$ (3.6 kcal mol^{-1} reported here). This already allows for different ligands to add at different rates, thereby removing the puzzle mentioned earlier.

For mechanism **A'** a similar but different reasoning is used: what matters here first is whether K_3 is smaller or bigger than 1, i.e. whether the triplet metal fragment would be present in solution mainly in its bare form, or as the triplet adduct. Except for the xenon adduct with $CpMn(CO)_2$, where K_3 is slightly larger than 1, K_3 is always much smaller than 1, so the reactant can be taken to be the free triplet fragment, and mechanism **A'** has two steps. Then, the apparent rate for solvent coordination depends on which step is rate-limiting. If the first step is rate-limiting, the observed rate constant should be k_{3a}, whereas if it is the second step, then the observed rate constant should be $K_3 k_{31}^{L}$. Again, the relative magnitude of the rate constants for disappearance of the intermediate, k_{3d} and k_{31}^{L} allow us to assign the predicted rate-limiting step. In this case, the second step is predicted to be rate-limiting for all solvents.

The final rows of Table 4 show the predicted overall rate constants for mechanisms **B** and **A'**. The larger predicted rate constant is presumed to correspond to the favoured mechanism. As can be seen, this varies from ligand to ligand, and for some ligands, the two predicted rates are similar, suggesting that both mechanisms can occur in parallel. Addition of heptane is however predicted to occur primarily through mechanism **A'**, due to strong binding of heptane even to $^3CpMn(CO)_2$, while for PFMCH, mechanism **B** is favoured. The predicted rate constants are in fair agreement with experiment, with xenon and carbon dioxide predicted to add ten times faster than observed, while C_7H_{14} and heptane are in even better agreement. This level of agreement is better than could be expected given the many uncertainties in the modelling.

Conclusions

In perfluoromethylcylohexane (PFMCH) we find that the conversion of $^3CpMn(CO)_2$ to $^1CpMn(CO)_2$(PFMCH) occurs much slower than the corresponding reactions in conventional alkanes. We measure the effect of the coordination ability by doping PFMCH with alkane, Xe and CO_2, leading to significant differences in the formation rates of $^1CpMn(CO)_2$(L) (L = alkane, Xe or CO_2) in PFMCH. We benchmark the ligand exchange by comparing these differences in rate with those observed for $^1CpRe(CO)_2$(PFMCH). The observation of differential rate of addition of different ligands to triplet

$CpMn(CO)_2$ is at first sight surprising given a proposed model[47] whereby in such cases, the rate of addition is driven by initial spin-state change in the metal fragment, and should therefore be ligand-independent. Here, we find that heptane adds to the manganese species *much* faster than does PFMCH, clearly showing that this model does not cover all possibilities. Instead, we propose a revised model (Figure 6) which allows for formation of metastable *triplet* adducts of the ligand to the metal fragment which can modulate the rate of spin state change. Based on DFT potential energy surface calculations and non-adiabatic transition state theory, we can then calculate rate constants for all the elementary steps in this mechanistic manifold, and predict overall rates. As shown in Table 4, these agree with experiment for all ligands within an order of magnitude, and reproduce the observed trend of much higher reactivity of heptane. The reason for this higher reactivity is the strong interaction between heptane and $CpMn(CO)_2$ in its triplet form, which favours the new revised mechanism.

Overall, the new experiments and calculations provide much additional insight into the mechanism of addition of ligands to high-spin metal centers, with the much more diverse pattern of reactivity of $CpMn(CO)_2$ compared to $Fe(CO)_4$ adding considerable new insight. This is valuable especially due to the importance of ligand addition and loss in organometallic chemistry, and the fact that these steps very often involve spin-state change.

Supporting Information

The supporting information contains additional details of the calculations, including a full list of Cartesian coordinates for all species.

Acknowledgements

We wish to thank EPSRC for funding to the Dynamic Structural Science (DySS) consortium at the Research Complex at Harwell (EP/ I01974X/1) and Central Laser Facility at the Rutherford Appleton Laboratory for access to the laser facilities. JNH and ZL acknowledge KU Leuven for funding through Grant No. C14/15/052. We gratefully acknowledge useful discussions with Professors M. Poliakoff and M. Towrie.

References

1. J. N. Harvey, *WIREs Comput. Mol. Sci.,* 2014, **4**, 1.
2. (a) M. Poliakoff, J. J. Turner, *J. Chem. Soc., Dalton Trans.*, 1973, 1351- 1357; (b) M. Poliakoff, J. J. Turner, *J. Chem. Soc., Dalton Trans.* 1974, 2276; (c) T. J. Barton, R. Grinter, A. J. Thomson, B. Davies, M. Poliakoff, *J. Chem. Soc., Chem. Commun.*, 1977, 841.
3. M. Poliakoff, *J. Chem. Soc., Dalton Trans.*, 1974, 210.
4. (a) A. J. Ouderkirk, P. Wermer, N. L. Schultz, E. Weitz, *J. Am. Chem. Soc.*, 1983, **105**, 3354; (b) T. A. Seder, A. J. Ouderkirk, E. Weitz, *J. Chem. Phys.*, 1986, **85**, 1977; (c) D. M. Hayes and E. Weitz, *J. Phys. Chem.*, 1991, **95**, 2723; (d) R. J. Ryther, E. Weitz, *J. Phys. Chem.*, 1991, **95**, 9841; (e) R. J. Ryther, E. Weitz, *J. Phys. Chem.*, 1992, **96**, 2561; (f) E. Weitz, *J. Phys. Chem.*, 1994, **98**, 11256; (g) S. P. Church, F. W. Grevels, H. Hermann, J. M. Kelly, W. E. Klotzbucher, K. Schaffner, *J. Chem. Soc., Chem. Commun.*, 1985; 594; (f) P. T. Snee, C. K. Payne, S. D. Mebane, K. T. Kotz, C. B. Harris, *J. Am. Chem. Soc.*, 2001, **123**, 6909; J. P. Lomont, S. C. Nguyen, C. B. Harris, *Organometallics*, 2012, **31**, 3947; J. P. Lomont, S. C. Nguyen, C. B. Harris, *Acc. Chem. Res.*, 2014, **47**, 1634
5 S. A. Trushin, W. Fuss, K. L. Kompa, W. E. Schmid, *J. Phys. Chem. A*, 2000, **104**, 1997.
6 H. Ihee, J. Cao, A. H. Zewail, *Angew. Chem. Int. Ed.*, 2001, **40**, 1532.
7. (a) T. Lee, F. Benesch, Y. Jiang, C. G. Rose-Petruck, *Chem. Phys.*, 2004, **299**, 233; (b) B. Ahr, M. Chollet, B. Adams, E. M. Lunny, C. M. Laperle, C. Rose-Petruck, *Phys, Chem. Chem. Phys.*, 2011, **13**, 5590; (c) P. Wernet, K. Kunnus, I. Josefsson, I Rajkovic, W. Quevedo, M. Beye, S. Schreck, S. Grubel, M. Scholz, D. Nordlund, W. Zhang, R. W. Hartsock, W. F. Schlotter, J. J. TurnerB. Kennedy, F. Hennies, F. M. F. de Groot, K. J. Gaffney, S. Techert, M. Odelius, A. Fohlisch, *Nature*, 2015, **520**, 78; (b) K. Kunnus, S. Schreck, A. Fohlisch, *Journal of Electron Spectroscopy and Related Phenomena*, 2015, **204**, 345; (c) A. J. Atkins, M. Bauer, C. R. Jacob, *Phys. Chem. Chem. Phys.*, 2015 **17**, 13937; (e) K. Kunnus, I. Josefsson, I. Rajkovic, S. Schreck, W. Quevedo, M. Beye, C. Weniger, S. Grubel, M. Scholz, D. Nordlund, W. Zhang, R. W. Hartsock, K. J. Gaffney, W. F. Schlotter, J. J. Turner, B. Kennedy, F. Hennies, F. M. F. de Groot, S. Techert, M. Odelius, P. Wernet, A. Fohlisch, *Structural Dynamics*, 2016, **3**, 043204
8. T. Leitner, I. Josefsson, T. Mazza, P. S. Miedema, H. Schroder, M. Beye, K. Kunnus, S. Schreck, S. Dusterer, A. Fohlisch, A M. Meyer, M. Odelius, P. Wernet, *J. Chem. Phys.*, 2018, **149**, 044307.
9. M. K. Kuimova, W. Z. Alsindi, J. Dyer, D. C. Grills, O. S. Jina, P. Matousek, A. W. Parker, P. Portius, X. Z. Sun, M. Towrie, C. Wilson, C.; J. X. Yang, M. W. George, *Dalton Trans.*, 2003, 3996.
10. (a) P. Portius, Y. Yang, X. Z. Sun, D. C. Grills, P. Matousek, A. W. Parker, M. Towrie, M, W. George, *J. Am. Chem. Soc.*, 2004, **126**, 10713; (b) X. Z. Sun, P. Portius, D. C. Grills, A. J. Cowan, M. W. George, *Appl. Spectr.*, 2008, **62**, 24.
11. M. Besora, J. L. Carreon-Macedo, A. J. Cowan, M. W. George, J. N. Harvey, P. Portius, K. L. Ronayne, X. Z. Sun, M. Towrie, *J. Am. Chem. Soc.*, 2009, **131**, 3583.
12. M. Besora, J. L. Carreon-Macedo, A. Cimas, J. N. Harvey, *Adv. Inorg. Chem.*, 2009, **61**, 573.
13. P. T. Snee, H. Yang, K. T. Kotz, C. K.; Payne, C. B. Harris, *J. Phys. Chem. A*, 1999, **103**, 10426.
14. (a) H. Yang, M. C. Asplund, K. T. Kotz, M. J. Wilkens, H. Frei, C. B. Harris, *J. Am. Chem. Soc.*, 1998, **120**, 10154; (b) P. T. Snee, C. K. Payne, K. T. Kotz, H. Yang, C. B. Harris, *J. Am. Chem. Soc.*, 2001, **123**, 2255.
15. C. Hall, W. D. Jones, R. J. Mawby, R. Osman, R. N. Perutz, M. K. Whittlesey, *J. Am. Chem. Soc.*, 1992, **114**, 7425; (b) S. A. Macgregor, O.Eisenstein, M. K. Whittlesey, R. N. Perutz, J. *Chem. Soc., Dalton Trans.*, 1998, 291.
16. E.A. Glascoe, K. R. Sawyer, J. E. Shanoski, C. B. Harris, *J. Phys. Chem. C*, 2007, **111**, 8789.
17. (a) A. A. Bengali, R. G. Bergman, C. B. Moore, *J. Am. Chem. Soc.*, 1995, **117**, 3879; (b) P. E. M. Siegbahn, *J. Am. Chem. Soc.*, 1996, **118**, 1487.
18. (a) R. D. Rimmer, D. C. Grills, H. Fan, P. C. Ford, K. G. Caulton, *J. Am. Chem. Soc.*, 2008, **129**, 15430; (b) M. J. Ingleson, M. Pink, H. Fan, K. G. Caulton, *J. Am. Chem. Soc*., 2008, **129**, 4262.
19. C. R. Kemnitz, E. S. Ball, R. J. McMahon, *Organometallics*, 2012, **31**, 70.
20. B. Rábay, T. Braun and J. P. Falkenhagen, *Dalton Trans*., 2013, **42**, 8058.
21. (a) J. M. Kelly, C. Long, R. Bonneau, *J. Phys. Chem.*, 1983, **87**, 3344; (b) R. Bonneau, J. M. Kelly, *J. Am. Chem. Soc*., 1980, **102**, 1220.
22. R. N. Perutz, J. J. Turner, *J. Am. Chem. Soc*., 1975, **97**, 4791.
23. C. Hall, R. N. Perutz, *Chem. Rev*., 1996, **96**, 3125.
24. R. D. Young, *Chem. Eur. J.*, 2014, **20**, 12704.
25. (a) X-Z. Sun, S. M. Nikiforov, D. C. Grills, M. Poliakoff, M. W. George, *J. Am. Chem. Soc.*, 1997, **119**, 7521; (b) G. E. Ball, T. Darwish, S. Geftakis, M. W. George, D. J. Lawes, P. Portius, J. P. Rourke, *Proc. Nat. Acad. Sci.*, 2005, **102**, 1853.
26. (a) D. J. Lawes, S. Geftakis, G. E. Ball, *J. Am. Chem. Soc.,* 2005, **127**, 4134; (b) D. J. Lawes, T. A. Darwish, T. Clark, J. B. Harper, G. E. Ball, *Angew. Chem., Int. Ed.,* 2006, **45**, 4486; (c) G. E. Ball, C. M. Brookes, A. J. Cowan, T. A. Darwish, M. W. George, H. K. Kawanami, P. Portius, J. P. Rourke, *Proc. Natl. Acad. Sci.,* 2007, **104**, 6927; (d) S. B. Duckett, M. W. George, O. S. Jina, S. L. Matthews, R. N. Perutz, X.-Z.. Sun, K. Q Vuong, *Chem. Commun*., 2009, 1401; (e) W. H. Bernskoetter, C. K. Schauer, K. I. Goldberg, M. Brookhart, *Science*, 2009, **326**, 553; (f) J. A. Calladine, O. Torres, M. Anstey, G. E. Ball, R. G.; Bergman, J. Curley, S. B. Duckett, M. W. George, A. I. Gilson, D. J. Lawes, R. N. Perutz, X.-Z. Sun, P. C. Vollhardt, *Chem. Sci.*, 2010, **1**, 622; (g) R. D. Young, A. F. Hill, W. Hillier, G .E. Ball, *J. Am. Chem. Soc.,* 2011, **133**, 13806; (h) R. D. Young, D. J. Lawes, A. F. Hill, G. E. Ball, *J. Am. Chem. Soc*., 2012, **134**, 8294-8297; (i) J. A. Calladine, S. B. Duckett, M. W. George, S. L. Matthews, R. N. Perutz, O. Torres, K. Q. Vuong, *J. Am. Chem. Soc.,* 2011, **133**, 2303; (j) O. Torres, J. A. Calladine, S. B.

Duckett, M. W. George, R. N. Perutz, *Chem. Sci.*, 2015, **6**, 418; (k) H. M. Yau, A. I. McKay, H. Hesse, R. Xu, M. He, C. E. Holt, G. E. Ball, *J. Am. Chem. Soc.*, 2016, **138**, 281.
27. (a) S. D. Pike, A. L. Thompson, A. G. Algarra, D. C. Apperley, S. A. Macgregor, A. S. Weller, *Science*, 2012, **337**, 1648; (b) S. D. Pike, F. M. Chadwick, N. H. Rees, M. P. Scott, A. S. Weller, T. Krämer, S. A. Macgregor, *J. Am. Chem. Soc.,* 2015, **137**, 820; (c) F. M. Chadwick, N. H. Rees, A. S. Weller, T. Krämer, M. Iannuzzi, S. A. Macgregor, *Angew. Chem., Int. Ed.,* 2016, **55**, 3677; (d) A. I. McKay, T. Kramer, N. H. Rees, A. L. Thompson, K. E. Christensen, S. A. Macgregor, A. S. Weller, *Organometallics*, 2017, **36**, 22; (e) F. M. Chadwick, A. I. McKay, A. J. Martinez-Martinez, N. H. Rees, T. Krämer, S. A. Macgregor, A. S. Weller, *Chem. Sci.,* 2017, **8**, 6014.
28. S. A. Bartlett, N. A. Besley, A. J. Dent, S. Diaz-Moreno, J. Evans, M. L. Hamilton, M. W. D. Hanson-Heine, R.Horvath, V. Manici, X.-Z. Sun, M. Towrie, L. Wu, X. Zhang, M. W. George, *J. Am. Chem. Soc.*, 2019 *in press*.
29. S. Seidel, K. Seppelt, *Science* 2000, **290**, 117.
30. (a) X-Z. Sun, M. W. George, S. G. Kazarian, S. M. Nikiforov, M. Poliakoff, *J. Am. Chem. Soc.,* 1996, **118**, 10525; (b) G. I., Childs, C. S. Colley, J. Dyer, D. C. Grills, X.-Z. Sun, J. Yang, M. W. George*, J. Chem. Soc. Dalton Trans.*, 2000, 1901; (c) D. C. Grills, M. W. George, *Adv. Inorg. Chem.,* 2001, **52**, 113; (d) O. S. Jina, X. Z. Sun, M. W. George, *Dalton Trans.,* 2003, 1773.
31. G. I. Childs, D. C. Grills, X. Z. Sun and M. W. George, *Pure and Appl. Chem.*, 2001, **73**, 443-447.
32. G. E. Ball, T. Darwish, S. Geftakis, M. W. George, D. J. Lawes, P. Portius, J. P. Rourke, *Proc. Nat. Acad. Sci.,* 2005, **102**, 1853.
33. K. K Pandey, *Coord. Chem. Rev*., 1995, **140**, 37.
34. I. Castro-Rodriguez, H. Nakai, L. N. Zakharov, A. L. Rheingold, K. Meyer, *Science,* 2004, **305**, 1757.
35. J. Yang, B. Nguessan, A. Dedieu, D. C. Grills, X.-Z. Sun, M. W. George, *Organometallics*, 2009, **28**, 3113.
36. J. A. Calladine, K. Q. Vuong, X.- Z. Sun, M. W. George, *Pure and Appl. Chem.,* 2009, **81**, 1667.
37. R. P. Hughes, H. A. Trujillo, *Organometallics*, 1996, **15**, 286.
38. P. Brennan, M. W George, O. S. Jina, C. Long, J. McKenna, M. T. Pryce, X. Z. Sun, K. Q.; Vuong, *Organometallics,* 2008, **27**, 3671.
39. G. M. Greetham, P. Burgos, Q. Cao, I. P. Clark, P. S. Codd, R. C. Farrow, M. W. George, M. Kogimtzis, P. Matousek, A. W. Parker, M. R. Pollard, D. A. Robinson, Z.-J. Xin, M. Towrie, *Appl. Spectrosc.,* 2010, **64**, 1311.
40. Gaussian 09, Revision D, M. J. Frisch, G. W. Trucks, H. B. Schlegel, G. E. Scuseria, M. A. Robb, J. R. Cheeseman, G. Scalmani, V. Barone, G. A. Petersson, H. Nakatsuji, X. Li, M. Caricato, A. Marenich, J. Bloino, B. G. Janesko, R. Gomperts, B. Mennucci, H. P. Hratchian, J. V. Ortiz, A. F. Izmaylov, J. L. Sonnenberg, D. Williams-Young, F. Ding, F. Lipparini, F. Egidi, J. Goings, B. Peng, A. Petrone, T. Henderson, D. Ranasinghe, V. G. Zakrzewski, J. Gao, N. Rega, G. Zheng, W. Liang, M. Hada, M. Ehara, K. Toyota, R. Fukuda, J. Hasegawa, M. Ishida, T. Nakajima, Y. Honda, O. Kitao, H. Nakai, T. Vreven, K. Throssell, J. A. Montgomery, Jr., J. E. Peralta, F. Ogliaro, M. Bearpark, J. J. Heyd, E. Brothers, K. N. Kudin, V. N. Staroverov, T. Keith, R. Kobayashi, J. Normand, K. Raghavachari, A. Rendell, J. C. Burant, S. S. Iyengar, J. Tomasi, M. Cossi, J. M. Millam, M. Klene, C. Adamo, R. Cammi, J. W. Ochterski, R. L. Martin, K. Morokuma, O. Farkas, J. B. Foresman, and D. J. Fox, Gaussian, Inc., Wallingford CT, 2016.
41. F. Weigend, R. Ahlrichs, *Phys. Chem., Chem. Phys.,* 2005, **7**, 3297.
42. J. N. Harvey, M. Aschi, H. Schwarz ,W. Koch, *Theor. Chem. Acc.*, 1998, **99**, 95.
43. R. F. Ribeiro, A. V. Marenich, C. J. Cramer, D. G. Truhlar, *J. Phys. Chem. B*, 2011, **115**, 14556.
44. D. R. Glowacki, C.-H. Liang, C. Morley, M. J. Pilling, S. H. Robertson, *J. Phys. Chem. A,* 2012, **116**, 9545.
45. H.-J. Werner, P. J. Knowles, G. Knizia, F. R. Manby, M. Schütz, *WIREs Comput. Mol. Sci.,* 2012, **2**, 242.
46. J. N. Harvey, M. Aschi, *Faraday Disc.*, 2003, **124**, 129.
47. D. Schott, P. Callaghan, J. Dunne, S. B. Duckett, C. Godard, J. M. Goicoechea, J. N. Harvey, J. P. Lowe, R. J. Mawby, G. Müller, R. N. Perutz, R. Poli, M. K. Whittlesey, *Dalton Trans.*, 2004, 3218.
48. L. E. Rush, P. G. Pringle, J. N. Harvey, *Angew. Chem., Int. Ed.*, 2014, **53**, 8672.
49. S. Essafi, J. N. Harvey, *J. Phys. Chem. A*, 2018, **122**, 3535.